A Versatile Magnetorquer Design for Microsatellite Constellation Missions

Philip R. Hampton
Space Flight Laboratory, University of Toronto Institute for Aerospace Studies
4925 Dufferin Street, Toronto, Ontario, Canada, M3H 5T6
phampton@utias-sfl.net

Faculty Advisor: Dr. Robert E. Zee
Space Flight Laboratory, University of Toronto Institute for Aerospace Studies

ABSTRACT

Attitude determination and control hardware for small satellites is constantly transforming to improve pointing accuracy and stability for target tracking missions. Magnetic attitude control is an effective and inexpensive approach when developing microsatellites for low earth orbit constellation missions. The Space Flight Laboratory (SFL) has implemented magnetic torquers (magnetorquers) and permanent magnets in previous missions for active and passive magnetic attitude control. A magnetorquer generates a magnetic dipole that torques the spacecraft when in the presence of Earth's magnetic field. This paper outlines the design, analysis, and testing of an embedded coil magnetorquer for SFL's SPARTAN and DEFIANT platforms. The SPARTAN magnetorquer was designed to be easily adaptable to other SFL platforms, including the DEFIANT platform which is shown to have only minor modifications. Simulations of sample missions for both platforms show how the magnetorquers are able to detumble the spacecraft after launch vehicle separation as well as mitigate reaction wheel saturation. All flight magnetorquers must go through environmental acceptance testing before they are ready for spacecraft integration. A set of three identical magnetorquers are orthogonally mounted in their respective platforms to enable magnetic dipole generation in all three body axes.

I. INTRODUCTION

The NewSpace revolution has seen many organizations competing to launch multiple satellites at an aggressive rate while continuously innovating their technology and product offerings. Optimizing the scale of constellations with accelerated assembly and testing while maintaining a robust and inexpensive design is crucial to mission feasibility and success for small satellites. Current missions and proposals for Low Earth Orbit (LEO) satellite constellations are in place to create a low latency global internet, even in remote areas. In addition, LEO satellite constellations are fulfilling geolocation and Earth observation operations for commercial and military applications. Many of these missions require precise knowledge of the orbit position as well as strict pointing requirements during target tracking. The Attitude Determination and Control Subsystem (ADCS) is responsible for orienting the spacecraft in the desired positon for uninterrupted payload operations. The attitude hardware, consisting of sensors and actuators, are interfaced with an on-board computer to determine the current attitude and subsequent torque outputs for obtaining the desired attitude.

Methods using Earth's magnetic field for attitude determination and control are well established in small satellites. The Space Flight Laboratory (SFL) has implemented magnetic attitude control in many of their previously launched small satellites. In particular, the CanX-7 Automatic Dependent Surveillance – Broadcast (ADS-B) and drag sail deorbiting demonstration mission uses a single sensor (three-axis magnetometer) and three orthogonally mounted magnetorquers for magnetic only attitude determination and control [1]. Satellites in LEO take advantage of the geomagnetic field strength to estimate the local magnetic field vector in the body frame of reference with a magnetometer, and torque the spacecraft with magnetic dipoles generated from the magnetorquers. Acting alone, magnetorquers are only capable of two-axis control as they have no authority about Earth's magnetic field line. Therefore, orbital parameters play an important role in the magnetic capabilities of the ADCS as the rate of change of Earth's magnetic field (B-dot) over time varies with the inclination. Even though precise three-axis control is not practical using only magnetorquers, a greater change in the external magnetic field direction over the course of an orbit increases the overall magnetic attitude control coverage of a spacecraft. The spacecraft experiences a maximum torque when the magnetic dipole is orthogonal to the magnetic field direction. A satellite in an equatorial orbit experiences a nearly constant magnetic

field, with a slight change over time due to the small offset of the geomagnetic poles from the geographic poles. Most SFL missions are designed for low-altitude Sun-Synchronous Orbits (SSOs) which have fairly high inclinations, making them ideal for magnetic attitude determination and control with the variation in the geomagnetic field direction. The SSO plane precesses at the same rate that the Earth rotates around the Sun by taking advantage of the natural nodal regression from J2 effects [2].

Two types of magnetorquers commonly used for space applications are torque rods and embedded coils in a Printed Circuit Board (PCB). Both utilize coil loops over an average area that generates a magnetic dipole along the axis of the loops when electric current flows through the coils. A torque rod is the most efficient way of maximizing the magnetic dipole magnitude per unit volume, but there are some disadvantages for use on small satellites. Compared to a PCB design, a torque rod can have a greater mass and cause hysteresis effects when equipped with a ferromagnetic core. Small satellites usually do not require significant magnetic dipole strength for attitude control, which makes a custom PCB magnetorquer a viable solution. A custom PCB offers a design to fit flat against the supporting structure of a spacecraft, manufacturing is repeatable and reliable, and it is considerably inexpensive when dealing with the scale of constellation missions.

This paper details the design, analysis, and testing of two PCB magnetorquers for the SPARTAN and DEFIANT platforms. Both SFL platforms are designed for constellation missions and are equipped with three identical magnetorquers.

II. BACKGROUND

Spacecraft Attitude Dynamics

The ADCS of a spacecraft implements control algorithms that read sensors and enable actuators to achieve a desired attitude, satisfying the pointing requirements of a mission. For a rigid spacecraft with three orthogonal reaction wheels, the motion expressed in the body frame is governed by Euler's equation:

$$\boldsymbol{I_b}\dot{\boldsymbol{\omega}}_b + \boldsymbol{\omega}_b{}^\times(\boldsymbol{I_b}\boldsymbol{\omega}_b + \boldsymbol{h_w}) = \boldsymbol{\tau_c} + \boldsymbol{\tau_d} \tag{1}$$

where $\boldsymbol{I_b}$ is the inertia matrix about the body's center of mass, $\boldsymbol{\omega}_b$ is the body's angular velocity, $\boldsymbol{h_w}$ is the angular momentum of the reaction wheels, $\boldsymbol{\tau_c}$ is the control torque, and $\boldsymbol{\tau_d}$ is the environmental disturbance torque [3].

Many SFL platforms use a set of orthogonally mounted reaction wheels to enable precise target tracking for payload operations, ground station data transfers, and sun pointing attitudes for optimizing power generation. Over time, the wheels accumulate and store angular momentum while compensating for disturbance torques acting on the spacecraft, as shown in Equation 2.

$$\Delta\boldsymbol{h_w} = \int_{t_o}^{t_f} \boldsymbol{\tau_d}\, dt \tag{2}$$

In order to avoid wheel saturation, magnetorquers take advantage of Earth's magnetic field to efficiently remove stored wheel momentum. This can be done through momentum dumping where certain fractions of each orbit are dedicated to wheel desaturation. Momentum management is a more continuous approach that removes stored wheel momentum over an orbit without disrupting the desired attitude state. In each case, the control torque on the spacecraft from the magnetorquers must be greater than the environmental disturbance torques in order to keep the reaction wheels functional.

Environmental Disturbance Torques

In LEO, there are four main environmental disturbance torques that should be considered: magnetic field, solar radiation pressure, aerodynamic, and gravity gradient [4].

The magnetic field torque experienced by a spacecraft is calculated using Equation 3:

$$\boldsymbol{\tau_B} = \boldsymbol{m_r}^\times \boldsymbol{B} \tag{3}$$

where $\boldsymbol{m_r}$ is the residual (parasitic) magnetic dipole of the spacecraft and $\boldsymbol{B}$ is Earth's magnetic field. The residual magnetic dipole has contributions primarily from solar panels, reaction wheels, and current flowing in the wiring harness, but can severely increase in magnitude with the addition of a ferromagnetic material for passive attitude control. The following equation is used to determine the geomagnetic field strength:

$$B = \lambda \frac{M}{a^3} \tag{4}$$

where λ is the magnetic latitude coefficient, M is the magnetic dipole strength of Earth, and a is the orbit semi-major axis. The latitude coefficient ranges from 1 at the magnetic equator to 2 at the magnetic poles.

The solar radiation pressure torque is calculated by the following cross-product:

$$\boldsymbol{\tau_s} = \boldsymbol{r_s}^\times \boldsymbol{F_s} \tag{5}$$

where $\boldsymbol{r_s}$ is the distance from the spacecraft center of mass to the center of solar pressure and $\boldsymbol{F_s}$ is the solar

radiation force. Solar radiation pressure (p_s) creates a force on the spacecraft that depends on the projected frontal area (A_p) with respect to the sun vector ($\boldsymbol{s}$) and the solar radiation pressure coefficient (C_p) of the exposed spacecraft surface, shown in Equation 6.

$$\boldsymbol{F}_s = p_s C_p A_p (-\hat{\boldsymbol{s}}) \tag{6}$$

The radiation pressure coefficient varies from 1 having complete absorption to 2 having complete reflection.

Similarly, the aerodynamic torque is the cross-product of a center of mass offset and an external force:

$$\boldsymbol{\tau}_a = \boldsymbol{r}_a^\times \boldsymbol{F}_a \tag{7}$$

where $\boldsymbol{r}_a$ is the distance from the spacecraft center of mass to the center of aerodynamic pressure and $\boldsymbol{F}_a$ is the aerodynamic force. The aerodynamic force factors in Earth's rotation, as the applied direction is opposite to the relative velocity ($\boldsymbol{V}_r$) of the spacecraft with respect to the atmosphere, and is calculated from the following equation:

$$\boldsymbol{F}_a = \frac{1}{2} D C_D A_p V_r^2 (-\hat{\boldsymbol{V}}_r) \tag{8}$$

where D is the atmospheric density and C_D is the spacecraft drag coefficient.

Lastly, the gravity gradient torque on a spacecraft can be determined using Equation 9:

$$\boldsymbol{\tau}_g = 3 \frac{\mu_E}{a^3} \boldsymbol{r}_b^\times I_b \boldsymbol{r}_b \tag{9}$$

where μ_E is the Earth gravitational parameter and $\boldsymbol{r}_b$ is the spacecraft orbital position (radius).

The magnetic dipole strength requirement of a magnetorquer is determined by using the lowest theoretical orbit altitude for the respective platform and assumes all of the worst-case disturbance torques act on a spacecraft in the same direction at the same time. This conservative approach ensures the magnetorquer can overcome the combination of disturbance torques in any attitude or orbit position. In reality, the disturbance torques can either combine or cancel out over the course of an orbit. For instance, Figure 1 shows how the magnetic field vector over three orbits is quasi-periodic in all three body axes when holding a fixed inertial attitude. Therefore, the average torque from the external magnetic field over an orbit approaches zero if an inertial attitude is held during nominal operations. A target-tracking or sun pointing mission will see more arbitrary external torques over an orbit, making momentum management a more suitable control technique. Hence,

designing a magnetorquer that can generate an average torque greater than the worst-case combination of disturbance torques enables continuous magnetic attitude control. Increasing the magnetic dipole strength improves the efficiency of reaction wheel desaturation and spacecraft detumbling.
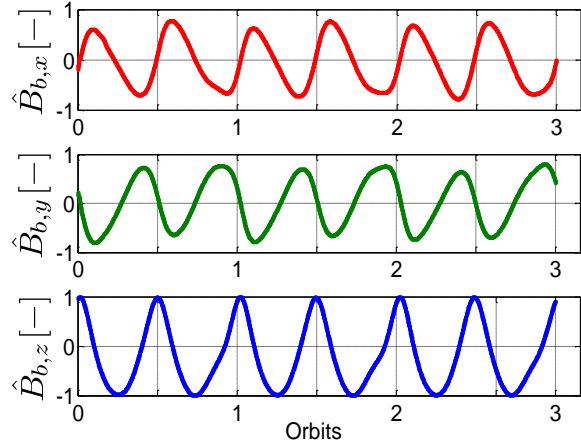

Figure 1: Normalized Magnetic Field Vector in the Spacecraft Body Frame - Inertial Attitude
[525km SSO, 1500 LTAN, Summer Solstice]

Magnetic Attitude Control

Controlling the spacecraft's attitude and angular velocity with magnetorquers is achieved by generating a magnetic dipole that interacts with Earth's magnetic field. The expected magnetic dipole of a magnetorquer is determined by the following equation:

$$\boldsymbol{m}_m = IAN \tag{10}$$

where I is the current, $\boldsymbol{A}$ is the area vector, and N is the number of coil windings. A PCB magnetorquer has a vacuum-core electromagnetic coil embedded in a dielectric material. Figure 2 shows how the current direction in the copper coils of a PCB influences the direction of the magnetic dipole (following the right-hand rule), which is normal to the plane of the board.
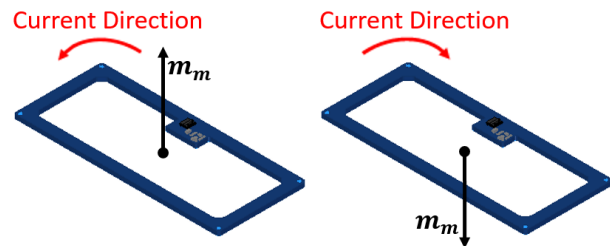

Figure 2: Magnetic Dipole Direction of a Printed Circuit Board Magnetorquer

Increasing the overall dimensions of a PCB and maximizing the number of layers allows for more coil loops. Adding more coil loops increases the overall

length of the coil and total resistance, causing the current to decrease when connected to a constant voltage. A trade-off study compares the mechanical and electrical limitations when designing a magnetorquer with a sufficient magnetic dipole. It is advantageous to reduce the current draw as much as possible to minimize heat dissipation and power consumption. A magnetorquer that directly or indirectly satisfies all applicable mission, system, and subsystem level requirements is a small but important step in closing the spacecraft design.

The magnetorquer's magnetic dipole establishes a control torque in the same way the spacecraft's residual magnetic dipole causes a disturbance torque from Equation 3, as shown below.

$$\tau_m = m_m^\times B \tag{11}$$

The control authority of three orthogonally mounted magnetorquers is limited by the direction of the geomagnetic field. If the coil axis of a magnetorquer is aligned with the external magnetic field, it is unable to produce a torque. At the same time step, the other two coil axes orthogonal to the magnetic field have the ability to produce a maximum torque. If the geomagnetic field direction is known, reaction wheel momentum management or coarse attitude control can be performed by regulating each of the magnetorquer's states using a closed-loop system.

A magnetometer is commonly used as a sensor in the ADCS as it determines the real-time geomagnetic field vector in the spacecraft body frame. The International Geomagnetic Reference Field (IGRF) model can be used in the flight code to compare the measured and expected magnetic field for calibration purposes. The magnetic field in the body frame varies due to the changing geomagnetic field as a function of orbital position, which is also constantly changing. Moreover, the angular velocity of the spacecraft also causes the local magnetic field in the body frame to change. Assuming the latter causes a higher rate of change in the local magnetic field vector (like when a spacecraft separates from the launch vehicle with tip-off body rates), a control algorithm using only the change in the local magnetic field over time (B-dot) can be executed to dampen body rates.

B-dot control simply uses the change in Earth's magnetic field to activate the magnetorquers:

$$m_m(t) = -K\dot{B}(t) \tag{12}$$

where K is the B-dot control gain [5]. This control law nulls angular rates with respect to the geomagnetic field line. In theory, the body rates do not completely converge to zero while in B-dot control as eventually one body axis will spin parallel to the magnetic field. On-

orbit, the change in position over time helps overcome this obstacle to reduce all three body rates, enabling the attitude control handover to the reaction wheels.

Theoretical Performance

Before a magnetorquer design is finalized, the theoretical performance can be predicted using electrical relationships. The resistance of the magnetorquer coil can be found using the following equation:

$$R = \frac{\rho N L_C}{A_C} \tag{13}$$

where ρ is the copper resistivity, N is the number of coil windings, L_C is the average coil length per layer, and A_C is the cross-sectional area of the coil (width by thickness of the copper trace). The magnetorquer current draw can then be calculated by following Ohm's Law:

$$I = \frac{V}{R} \tag{14}$$

where V is the regulated voltage from the power supply. Finally, Equation 10 uses the current draw to solve for the expected magnetic dipole of the PCB design.

In LEO, the spacecraft may experience a wide range of temperatures depending on the eclipse fraction. An effective thermal control system will keep the magnetorquers within their operating temperature range at all times, regardless of the spacecraft's attitude or mode of operation. The magnetic dipole generated by the magnetorquer can be predicted for the full range of operating temperatures by calculating how the resistivity of copper changes with respect to temperature:

$$\rho(T) = \rho_0[1 + \alpha(T - T_0)] \tag{15}$$

where T is the temperature of the copper, ρ_0 is the copper resistivity at the reference temperature, α is the temperature coefficient of copper, and T_0 is the reference temperature. The magnetorquer performance will degrade as the temperature of the PCB rises, which in turn decreases the reaction wheel desaturation efficiency. Since the worst-case combination of disturbance torques already has layers of conservatism in the analysis, only the nominal magnetic dipole is considered for the design requirement. This includes the assumption that all disturbance torques act in the same direction at the same time, which is highly unlikely. Therefore, the risk of the attitude state being compromised due to reaction wheel saturation during nominal operations is mitigated in any orbital position.

The final magnetorquer design for each of the small satellite platforms in the following section were

completed from evaluating trades between several subsystems, with the structure and layout of each platform presenting the leading design challenge.

III. MAGNETORQUER DESIGN

The two magnetorquer designs presented in this paper are for SFL's SPARTAN (6-12 kg) and DEFIANT (20-50 kg) platforms [6]. The SPARTAN platform follows a 6U XL nanosatellite form factor with a completely customized structure while being compatible with commercial launch vehicle deployment systems. The 6U XL bus in Figure 3 shows the SPARTAN model with articulating solar panels developed by SFL for high-power payloads.
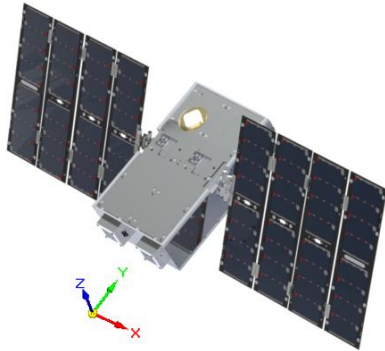
Figure 3: SPARTAN Deployed Configuration

The DEFIANT platform is a 36x36x45cm microsatellite developed by SFL primarily for constellation missions. Figure 4 illustrates the DEFIANT platform in its deployed configuration. The spacecraft is designed with a rapid Assembly, Integration, and Test (AIT) approach: implementing a triple internal-tray design to increase assembly efficiency and allow access to any component during integration. The DEFIANT platform is compatible with commercial separation systems and has the option of being equipped with deployable solar arrays to increase power generation for payload operations.
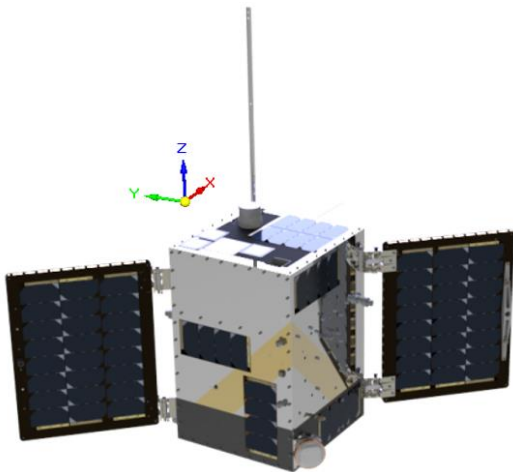

Figure 4: DEFIANT Deployed Configuration

Driving Requirements

The shared ADCS requirements for the SPARTAN and DEFIANT platforms that drive the magnetorquer design are listed in Table 1.

Table 1: Attitude Determination and Control Subsystem Requirements

Requirement	Description
ADCS-R001	The ADCS shall provide three-axis attitude determination and control capable of operating at 100% duty cycle.
ADCS-R002	The spacecraft shall generate sufficient power in the absence of active attitude control.
ADCS-R003	The ADCS shall be capable of detumbling the spacecraft from initial body rates determined from launch vehicle separation analysis.

Requirements ADCS-R001 and ADCS-R003 are satisfied by having three orthogonally mounted reaction wheels and magnetorquers capable of performing reaction wheel momentum management and B-dot control during worst-case tip-off rates. For the SPARTAN and DEFIANT platforms, a permanent magnet is needed to satisfy requirement ADCS-R002. If a spacecraft enters safehold mode, active attitude control is switched off resulting in a random tumble or inertial stare. The addition of a permanent magnet prevents undesirable attitudes to persist by having its magnetic dipole positioned along a designated spacecraft body vector. The torque caused by the permanent magnet forces the spacecraft into a passive tumble which provides a more spherical coverage of the sun on the body panels for sufficient power generation and thermal management. The direction of the permanent magnet in the spacecraft is determined through simulations when active attitude control is disabled. For thermal protection, the satellite must loadshed sufficiently early from bad attitudes that generate insufficient power for the permanent magnet to have its desired effect. Each requirement is verified through design and analysis, which is further discussed in Section IV. Attitude Simulations.

SPARTAN Design

To determine the strength of the magnetic dipole required for the SPARTAN magnetorquers, an estimate of the worst-case environmental disturbance torques was calculated. Figure 5 shows the total disturbance torque if all were to act in the same direction at the same time. The magnetic disturbance torque is far greater than the others with the addition of a permanent magnet. Conservative solar, atmospheric, and geomagnetic characteristics were used, as well as the lowest possible altitude from potential missions. This includes using a value of 2 for the radiation pressure coefficient and latitude coefficient as SSOs are fairly polar. The worst-case physical

properties of the spacecraft are also used, which includes a conservative maximum offset between the center of mass and center of pressures, and the largest possible projected frontal area with the articulating solar arrays.
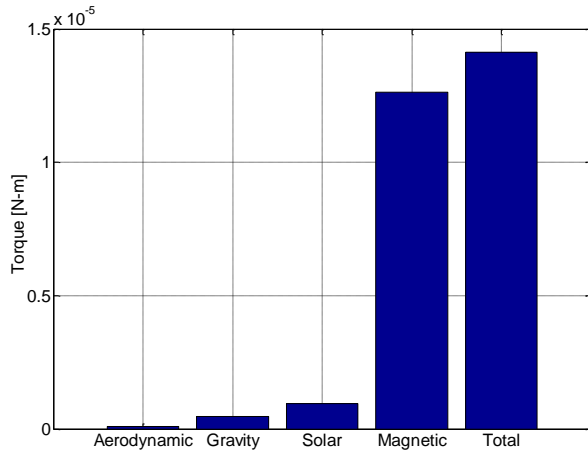

Figure 5: SPARTAN Platform Worst-Case Disturbance Torques

Having three identical magnetorquers for each spacecraft significantly reduces cost with the economy of scale. The identical magnetorquer design was heavily constrained by the mechanical fit on the SPARTAN platform. The three orthogonal positions illustrated in Figure 6 for the magnetorquers were proposed in the preliminary design phase.
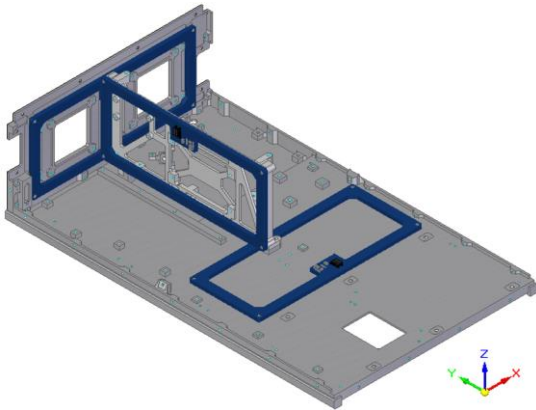
Figure 6: SPARTAN Magnetorquer Layout

After many iterations, the final compact design was able to fit in these locations with adequate clearance to all other flight components. This involved milling out the center of the PCB to make room for mounting other flight components and supporting structure. As demonstrated in Figure 6, the thickness of the PCB was also restricted by clearance constraints which limited the number of signal layers.

A small part of the board without coil loops was reserved to house the connector and electrical components. The size of this tab, located on the inner side of the coils, was severely limited by the structure and layout of the platform. In particular, the X and Y magnetorquer positions forced the tab size to be very compact, resulting in a challenging electrical component layout. A PCB is able to have electrical components soldered on either the top or bottom of the board. Since the bottom of the PCB is flush against the supporting structure, all of the components were forced to be on top without overlapping the coil loops. Figure 7 shows the +Y panel assembly and how the tab was only able to fit in the middle of the long side of the PCB as it is constrained by two indented bosses on both sides for mounting patch antennas on the external surface. Figure 8 shows the avionics bracket supporting the X magnetorquer and how the tab size is limited by the GPS receiver which is mounted directly below. The final design was able to densely pack the electrical components on the top of the tab along with a connector for the power and data lines.
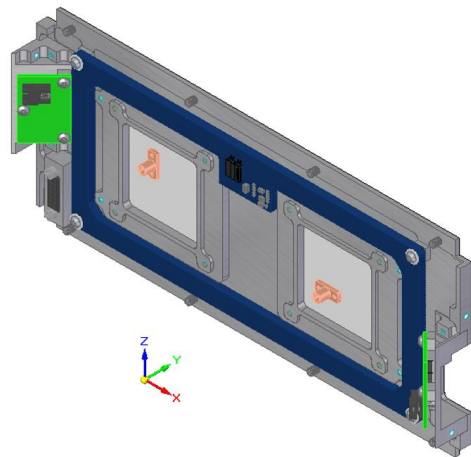

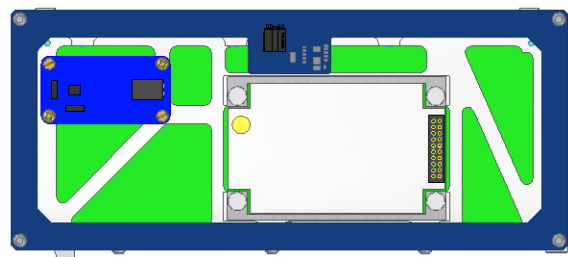**Figure 7: SPARTAN +Y Panel Assembly**

Figure 8: SPARTAN Avionics Bracket Assembly

The mechanical fit constraints of the PCB limited the number of coil loops as the board thickness did not allow for a design with the maximum number of signal layers. Increasing the board thickness by adding more layers would create inadequate clearance between other components which may cause damage during launch vehicle vibrations. The PCB has multiple coil loops per layer, as seen with the green traces in Figure 9. Each layer with coil loops is connected through a set of vias to its respective layers above and below. The top layer has

no coil loops as it connects the ends of the entire coil to the connector and provides power and data connections for the electrical components.
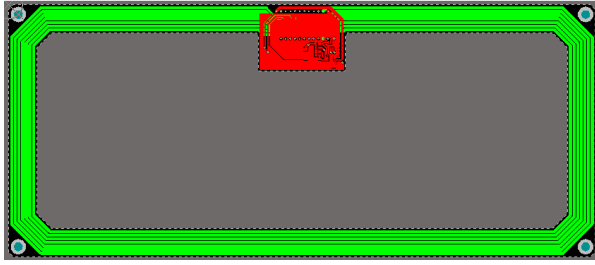

Figure 9: SPARTAN Magnetorquer Coil Loops

In order to decrease the power consumption and heat dissipation of the magnetorquer, the current draw was reduced as much as possible. With the average enclosed area of the coils determined by the size of the PCB and the voltage rail set, a trade-off study was analyzed in order to determine the number of coil loops per layer. With the thickness constraint limiting the number of coil loop layers, having seven coil loops with equal trace widths on each layer was deemed sufficient and met the magnetic dipole requirement. The nominal magnetic dipole of the SPARTAN magnetorquer at room temperature is $0.40 \, \text{Am}^2$, which creates a maximum torque of $1.82 \cdot 10^{-5}$ Nm using the same geomagnetic field strength and cross product angle that was used to determine the magnetic disturbance torque. Therefore, the generated torque from the magnetorquer is able to overcome the worst-case combination of disturbance torques ($1.41 \cdot 10^{-5}$ Nm).

The magnetorquer interfaces with the spacecraft through a four pin connector that has two power lines and two data lines. One of the electrical components on the tab is an H-bridge integrated circuit, which allows the current direction to be controlled. Since this component can get warm with constant use, a ground pour (shown in red in Figure 9) was implemented on the top layer to transfer heat to the coils and away from the tab. Table 2 shows the logic of how the two input data lines determine the magnetic dipole direction. Only the brake, forward, and reverse states are used in the flight code. The desired output state is determined by the Attitude Determination and Control Computer (ADCC) which activates the appropriate magnetorquers on-orbit.

Table 2: Magnetorquer States

| Input State | | Output State | Magnetic Dipole Direction |
Line 1	Line 2		
Low	Low	Brake	-
High	Low	Forward	North
Low	High	Reverse	South
High	High	Idle	-

DEFIANT Design

With the demonstrated Assembly, Integration and Testing (AIT) effectiveness and low cost of the SPARTAN magnetorquer, the design was modified to fit in the DEFIANT platform. Figure 10 shows the magnetorquer positions on the three structural body panels.
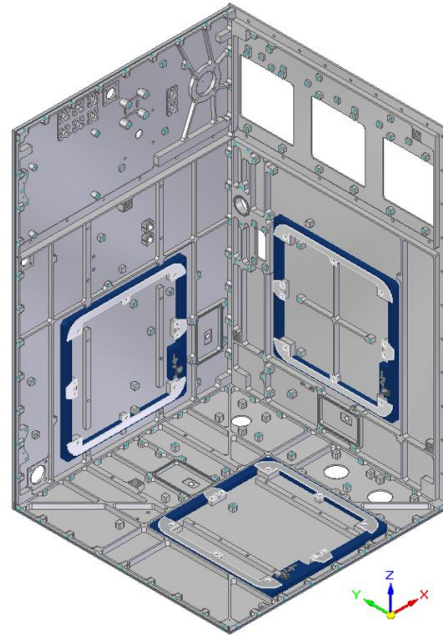

Figure 10: DEFIANT Magnetorquer Layout

The mechanical fit of the PCB was a little more flexible in the bigger platform but there was still a need to mill out the center of the board for mounting other avionics and wiring harness tie-down points. The three identical magnetorquers were adapted to the current design of each panel to reduce Non-Recurring Engineering (NRE) efforts. The magnetorquers are held in place with customized brackets instead of using the mounting holes on the four corners. Brackets were used for this platform as there was not enough room for bosses on the panels to have the minimum thread length needed for securing the magnetorquers with screws. If the magnetorquers were raised off the panels with adequate boss heights they would interfere with the internal trays and avionics. The increased boss height requirement compared to the SPARTAN platform was due to the placement of solar cell strings on the external surface of each body panel, as seen in Figure 4. The four mounting holes on the corners remained in the design in case other SFL platforms are able to implement this magnetorquer in future missions.

The electrical characteristics are very similar to the SPARTAN design, having seven coil loops per layer and the same trace cross-sectional area. To increase the total coil resistance, the number of PCB layers were maximized based on the reliable manufacturing limit.

Unlike in the SPARTAN design, there was not a strict thickness constraint for the PCB with the different mounting approach. Figure 11 illustrates how the tab size was increased to accommodate additional coil transfers between layers. The tab was also shifted to accommodate the mounting bracket locations. Moreover, the increased board thickness caused the via sizes to grow respecting the maximum aspect ratio capabilities of PCB manufacturers.
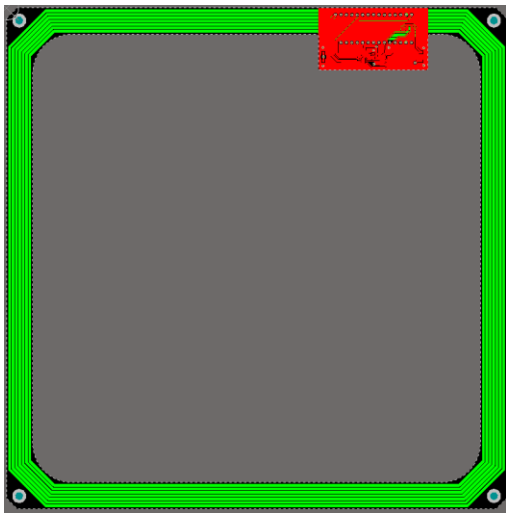

Figure 11: DEFIANT Magnetorquer Coil Loops

The spacecraft interface remains the same with the four output states available for attitude control. The same environmental disturbance torque analysis was performed using the worst-case orbit parameters and DEFIANT bus characteristics. The nominal magnetic dipole of the magnetorquer is 0.61 Am² which generates a maximum torque of $2.86 \cdot 10^{-5}$ Nm, which is greater than the conservative combination of worst-case disturbance torques ($1.99 \cdot 10^{-5}$ Nm) acting in the same direction at the same time. Many attitudes enable multiple magnetorquers to work together to generate a larger torque depending on the local magnetic field direction in the spacecraft body. In general, the control authority should be at least 2 times greater than the worst-case disturbance torque. Even though this is not the case along the magnetorquer axis for the SPARTAN and DEFIANT design when considering the conservative combination of disturbance torques, results from attitude simulations show a control authority greater than 2 times the maximum total disturbance torque using the same conservative orbit parameters.

IV.   ATTITUDE SIMULATIONS

Autonomous Guidance, Navigation, and Control (GNC) is achieved through the interface between sensors and actuators with feedback control implemented on the on-board computers. SFL has developed the MIRAGE attitude simulator which sets up an orbit environment while executing the flight code. In addition to the IGRF model for simulating the geomagnetic field, MIRAGE uses the Astronomical Almanac Sun Vector (AASV) to propagate the sun vector, Earth Gravitational Model (EGM), and International Astronomical Union 1976 (IAU-1976) model to provide knowledge of inertial and earth-fixed reference frame rotations. To set up an orbit, a Simplified General Perturbations (SPG4) model takes a Two-Line Element (TLE) set which propagates the spacecraft position from the specified epoch. For each mission, a script is developed with the spacecraft's characteristics and initial attitude state, including the moment of inertia about the center of mass and initial body rates. The script also contains all of the attitude hardware parameters to match the flight code. Furthermore, a simulation setup file is developed to provide MIRAGE with the attitude mode transitions at certain time steps.

MIRAGE simulations are used to verify ADCS requirements, including pointing accuracy and minimum slew rates for target tracking. The following simulations use theoretical orbit parameters each platform may encounter, with the lowest potential altitude used for conservative analysis. The B-dot control simulations are demonstrated with the SPARTAN platform and the momentum management simulations are demonstrated with the DEFIANT platform, even though similar analyses were conducted for both platforms. It is important to note that the magnetorquer control output torque in MIRAGE is generated by a fraction of the magnetic dipole magnitude at full current. In practice, a Pulse-Width Modulation (PWM) approach is used to fire the magnetorquer for a calculated fraction of each time step, as the current draw is fixed on a set voltage rail. For example, if the ADCC determines the desired current draw of the magnetorquer to be half of the nominal, the magnetorquer will be switched on for half of the time step. Filters are implemented in the magnetorquer design to attenuate Electromagnetic Interference (EMI) effects. This PWM approach produces very similar results to the MIRAGE simulations based on on-orbit data from previous SFL missions.

B-dot Control

The B-Dot control simulations shown in this subsection were executed using the bus characteristics and attitude hardware parameters of the SPARTAN platform. Since the articulating arrays can rotate about the x-axis, the inertia of the spacecraft is continuously updated with knowledge of the solar array drive mechanism angular position. During nominal operations of a sample mission, the solar arrays track the sun vector to optimize power generation while the payload antenna (-z face) tracks the ground targets. During B-dot control, the deployed arrays are stationary with the normal of each

array parallel with the z-axis. Requirement ADCS-R003 is verified through B-dot simulations where initial body rates are set for each axis in the script. The SPARTAN platform must be capable of detumbling tip-off body rates of up to 25°/s from launch vehicle separation, which was derived by analyzing compatible deployment systems and includes some margin. The simulation setup file sets the attitude mode to B-dot at the start of the simulation which activates only the three-axis magnetometer and set of magnetorquers. The magnetometer determines the difference in the magnetic field between each time step and dictates the desired magnetic dipole strength and direction of each magnetorquer. The B-dot control gain is set to a value that efficiently detumbles the spacecraft without causing unwanted over torqueing.

The B-dot simulation results shown for the SPARTAN platform are from a 525 km altitude, 15:00 Local Time of Ascending Node (LTAN) SSO that propagates from an epoch start date of June 21, 2020, 12:00:00 UTC. The simulation start time is set to 12:16:14 UTC of the same day, which is near the summer solstice. The simulation time span is set to run for three orbits. Figure 12 demonstrates rate damping with an initial angular velocity of 25°/s in the x-, y-, and z-axis, respectively, with the other axes having zero initial angular velocity.
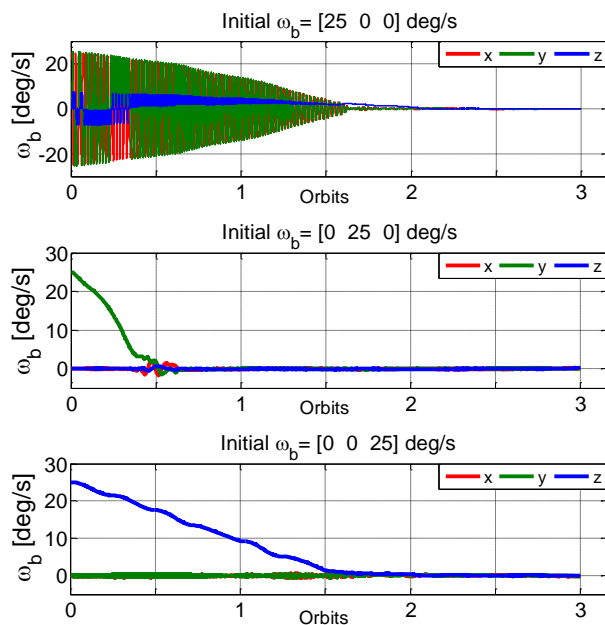

Figure 12: Body Rate Damping with B-dot Control after an Initial Tip-off Rate of 25°/s per Axis

An interesting outcome emerges from these results in regards to the spin stability of a spacecraft. The initial angular velocity in the x-axis causes the other axes to spin at a higher rate than the other two scenarios. This can be explained by the energy sink hypothesis, where a

quasi-rigid body will dissipate energy until a state of minimum kinetic energy is reached. Since the spacecraft is not entirely rigid and experiences small perturbations on-orbit, spins about the major axis of inertia are asymptotically stable and spins about the intermediate and minor axes are unstable. The articulating arrays of the SPARTAN platform deploy opposite from each other on the x-faces and have the following moments of inertia with the array faces normal to the z-axis: $I_{zz} > I_{xx} > I_{yy}$. Having an initial body rate on the intermediate or minor axis causes the body to nutate towards a major axis spin. Figure 12 shows how this causes a greater spike in the rates of the y-axis and z-axis when there is an initial body rate in the x-axis, which is the least stable axis. This also explains why the major-axis spin takes longer to dampen the body rates than a minor axis spin with the same initial angular velocity. A minor axis spin naturally dissipates energy until it reaches a minimum kinetic energy state, whereas a major axis spin resists change as it is already in a stable equilibrium. A major axis spin has more angular momentum, which furthermore explains why it takes longer to detumble as the angular acceleration is inversely proportional to the inertia with the same available control torque. After detumbling, the spacecraft eventually holds an attitude with the permanent magnet dipole direction tracking Earth's magnetic field line. As the solid model of the SPARTAN platform becomes more defined, it is expected that the products of inertia will increase causing a greater spike in the body rates that are initially set to zero for all cases.

A more likely scenario would have at least some initial body rates in all three axes after launch vehicle separation. Figure 13 shows the simulation results when all three body axes have an initial angular velocity of 15°/s, which is equivalent to a rate magnitude of 26°/s. After approximately 1.25 orbits, the spacecraft converges to a major axis spin before fully detumbling. All simulations show that the spacecraft can detumble itself from an initial angular velocity magnitude of 25°/s in less than two orbits: hence requirement ADCS-R003 is verified through simulation.
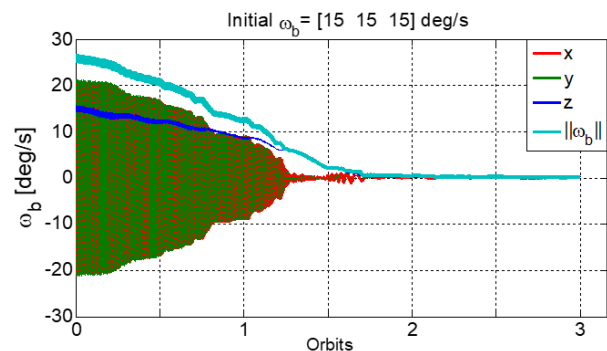

Figure 13: Body Rate Damping with B-dot Control after Initial Tip-off Rates of 15°/s in each Axis

Momentum Management

The reaction wheel momentum management simulations shown in this subsection were executed using the bus characteristics and attitude hardware parameters of the DEFIANT platform. The deployable arrays are non-articulating on the DEFIANT platform, so the moment of inertia about the center of mass remains constant. As seen in Figure 4, one side of the deployable arrays is covered in solar cells that maximize power generation when the angle of incidence is minimized between the sun vector and the array normal vector. For nominal operations of a sample mission, the simulation is set to be in target tracking mode during access times to a ground station in Svalbard. During the target tracking slew, the antenna boresight on the –z face is aligned with the ground target while the deployable array normal vector is constrained to the sun vector. Outside of the Svalbard access times, the array normal vector is aligned with the sun vector while the –z face is nadir constrained. The spacecraft is set to obtain the ground target 180 seconds before each access start time and hold for 30 seconds after each access end time. Requirement ADCS-R001 is verified through attitude hardware selection and simulations showing the magnetorquers are able to desaturate the reaction wheels as they accumulate angular momentum from disturbance torques. The simulation setup file regulates the attitude mode transition times while activating all of the sensors (magnetometer, sun sensors, rate sensor) and actuators (reaction wheels, magnetorquers). The Global Positioning System (GPS) antenna is also activated to sense orbital position, which has its boresight aligned closely with the normal of the deployable arrays to maximize reception. While the DEFIANT platform can accommodate a star tracker, it was not activated for this simulation. The initial body rates and reaction wheel speeds were set to zero.

The simulations results shown for the DEFIANT platform are from a 550 km altitude, 15:00 LTAN SSO that propagates from an epoch start date of December 21, 2019, 00:00:00 UTC. The simulation start time is set to 03:00:00 UTC of the same day, which is near the winter solstice. Figure 14 illustrates the environmental disturbance torques, magnetorquer output torque, and reaction wheel speeds over 10 orbits. The disturbance torques are greater in the x-axis and z-axis as the permanent magnet has its dipole in the +y direction. The greatest combined disturbance torque magnitude from the simulation is $1.38 \cdot 10^{-5}$ Nm, which is less than the worst-case value of $1.99 \cdot 10^{-5}$ Nm used for designing the magnetorquer's magnetic dipole. The magnetorquer control authority is approximately 2.1 times greater than the maximum disturbance torque in this simulation. The reaction wheels stay between +/- 450 rad/s, which is below the saturation limit of 700 rad/s.
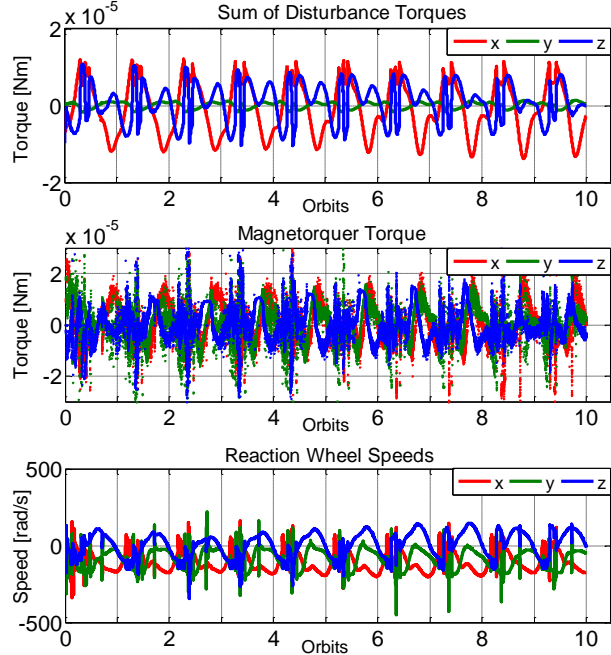

Figure 14: Momentum Management Simulation Results

Zooming in on a slew maneuver, Figure 15 demonstrates how the commanded output torque in the x-axis from the Y and Z magnetorquers counteracts the disturbance torques by mostly generating a torque in the opposite direction. This keeps the reaction wheels below their saturation speed limit and steady over time.
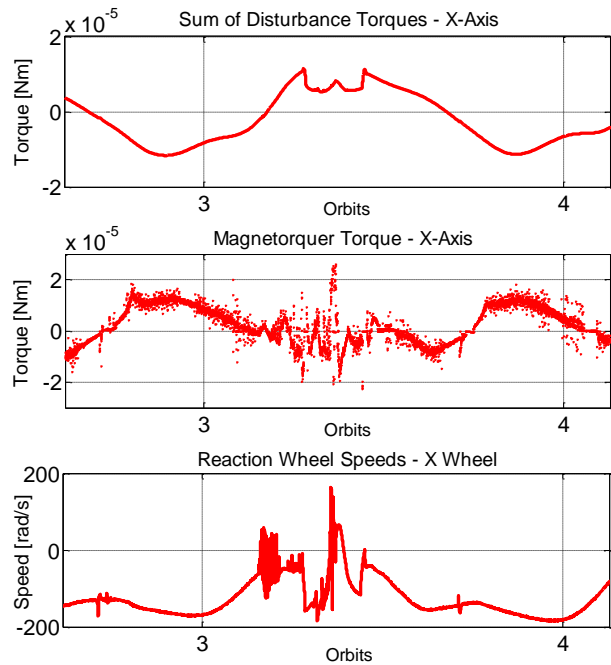

Figure 15: Momentum Management Simulation Results – X-Axis Comparison

Furthermore, Figure 16 shows the comparison of reaction wheel speeds with and without activated magnetorquers using the same simulation parameters. Without magnetorquers, the wheel speeds continue to grow as momentum accumulates from disturbance torques. When operating at the DEFIANT bus voltage, the reaction wheel control torque starts to decrease as wheel speeds rise above 600 rad/s [7]. The speed limit is set to 700 rad/s to ensure there is always sufficient control torque with appropriate margin. Increasing wheel speeds beyond 700 rad/s eventually causes the control torque to drop below its minimum limit, prematurely ending the mission if unable to desaturate.
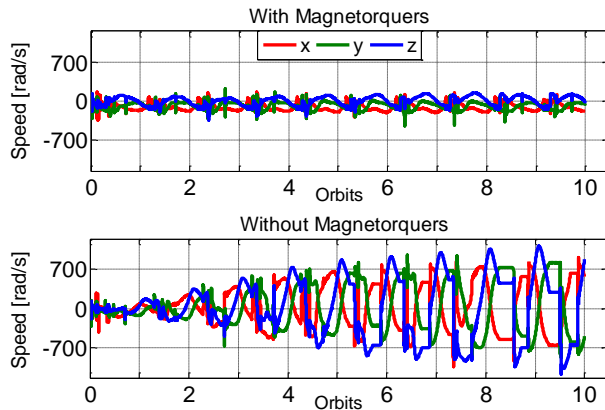

Figure 16: Reaction Wheel Speeds with and without Magnetorquers Activated

V. ACCEPTANCE TESTING

All flight magnetorquers must pass acceptance testing before they are approved for spacecraft integration. A flight ready magnetorquer will have passed a Long Form Functional Test (LFFT) at room temperature before and after thermal shock, as well as during thermal cycling. Before LFFTs commence, the mass of each magnetorquer is recorded for the system mass budget and mechanical fit checks are completed with the relevant spacecraft structure to confirm mounting compliance and adequate clearance.

Functional

The goal of the functional test is to confirm the four possible input states lead to the expected output states from Table 2 and the current draw in each state is as expected. The autotester board, shown in the top of Figure 17, can test up to 12 magnetorquers sequentially which is beneficial when working with the scale of constellation missions. To pass the functional test, the current draw in brake and idle should be less than 1 mA and the current draw in forward and reverse should be within 10% of the expected current derived from Equation 14. In addition, the initial functional test verifies polarity direction during the forward and reverse states with a compass.
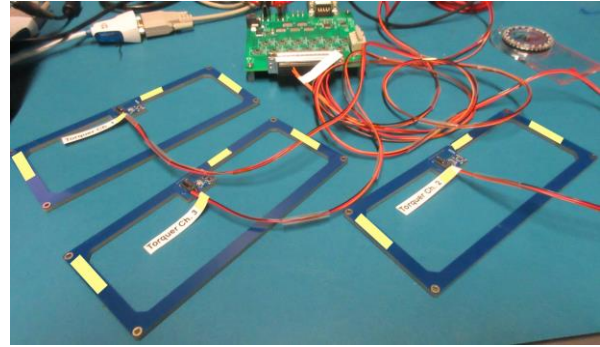

Figure 17: Functional Test with SFL's Autotester Board and Flight Set of SPARTAN Magnetorquers

Thermal Shock

The thermal shock test simulates a sudden change in temperature, which occurs when a spacecraft suddenly enters eclipse after being exposed to the sun, or vice versa. The purpose is to validate the workmanship on the solder joints of the electrical components on the PCB. The magnetorquer is transferred between two thermal chambers repeatedly: one set at the survival cold temperature, and the other set at the survival hot temperature. An inactive magnetorquer that exceeds survival temperatures is prone to damage. If a magnetorquer is turned on within its survival temperature limit but outside the operational temperature limit, significant damage could occur. During the thermal shock test, the magnetorquer itself never reaches its survival temperatures and is always off to eliminate any risk of unnecessary damage. Once the magnetorquer exceeds its operational temperature limit, it is transferred to the other chamber. The process of moving between thermal chambers is repeated 25 times, with temperature sensors monitoring the magnetorquer at all times. The magnetorquer is placed in antistatic bags with desiccant to protect from moisture caused by rapid changes in temperature. The desiccant is isolated from the unit under test to avoid contamination. A successful test shows no change to the solder joints after inspection. A functional test is performed after thermal shock to ensure the current draw in each of the four states has not changed.

Thermal Cycling

The purpose of the thermal cycling test is to ensure the magnetorquers function as expected across the full operating temperature envelope. The temperature profile is illustrated in Figure 18, with temperature sensors attached directly to the magnetorquers to monitor any inconsistencies between the thermal chamber control temperatures if they arise. All temperature soaks (plateaus in Figure 18) have a duration of one hour, with the temperature slew rate set to 2°C per minute to avoid additional thermal shocks.

Figure 18: Temperature Profile for Magnetorquer Thermal Cycling Testing

After the initial room temperature LFFT, the magnetorquers are turned off and brought up to soak at their survival hot temperature. The magnetorquers are then set to soak at their operational hot temperature before turning on and performing a LFFT. The same process is repeated for the survival and operational cold temperatures of the magnetorquers. The thermal chamber is then set to cycle between operational hot and cold temperatures while the autotester board continuously polls the current draw of each magnetorquer sequentially. The resulting current draw at each temperature is compared to expected values determined from the effect of temperature on copper resistivity (Equation 15). A final room temperature LFFT is performed at the end of thermal cycling to ensure that no significant change is found in the results from the initial room temperature LFFT.

Magnetic Field Measurement

The final test before a flight magnetorquer is accepted for spacecraft integration is measuring the magnetic field generated with a calibrated lab magnetometer. With a known current passing through the magnetorquer coils, the lab magnetometer measures the magnetic field along the coil's central axis using the measured differences between the active (forward and reverse) and inactive (brake and idle) states. Since the expected magnetic field is outside the range of SFL's lab magnetometer, the lab magnetometer is raised above the magnetorquer with a non-ferromagnetic support bracket. The expected magnetic field strength measured by the magnetometer can be estimated using the Biot-Savart Law:

$$B_m(z) = \frac{\mu_0 N I r_e}{2(r_e^2 + z^2)^{\frac{3}{2}}} \tag{16}$$

where z is the distance from the magnetorquer to the lab magnetometer measuring point along the central axis of the coils, μ_0 is the magnetic constant, N is the number of coil windings, I is the current, and r_e is the effective coil radius. The magnetorquer design is verified if the magnetic field measurement is within 10% of the predicted value. Following acceptance testing, each flight magnetorquer must accrue 1000 hours of burn-in testing to screen for premature failure (infant mortality).

VI. CONCLUSION

An uninterrupted attitude state while target tracking during payload operations or sun-tracking for optimizing power generation is essential for mission success. For LEO microsatellite constellation missions, taking advantage of the geomagnetic field for attitude determination and control can help lower costs and improve assembly and test efficiency. The versatile magnetorquer design presented in this paper shows how it can be adapted to fit on different SFL platform sizes without a significant redesign. Enabling the current in the coils to flow in either direction allows for dipole control in all three axes when three magnetorquers are mounted orthogonally in a spacecraft. The simulations show that the magnetorquers can overcome disturbance torques to dampen high body rates and remove accumulated angular momentum in the reaction wheels. ADCS requirements relevant to the magnetorquer were verified through design and analysis. A comprehensive environmental acceptance test was completed for each flight magnetorquer prior to spacecraft integration. The thorough analysis and testing of each magnetorquer plays an important role in closing the ADCS design which contributes to the robustness of SFL platforms.

VII. ACKNOWLEDGMENTS

VIII. REFERENCES

[1] B. Cotten, I. Bennett, and R. E. Zee, *On-Orbit Results from the CanX-7 Drag Sail Deorbit Mission*. SSC17-X-06, 2017.

[2] A. H. de Ruiter, C. Damaren, and J.R. Forbes, *Spacecraft Dynamics and Control: An Introduction*. John Wiley & Sons, Ltd, 2013.

[3] P. C. Hughes, *Spacecraft Attitude Dynamics*. Dover, 1986.

[4] J. R. Wertz, D. F. Everett, and J. J. Puschell, *Space Mission Engineering: The New SMAD*. Microcosm Press, 2011.

[5] A. Stickler and K. Alfriend, *An elementary magnetic attitude control system*. Journal of Spacecraft and Rockets, 1976.

[6] Space Flight Laboratory, "Satellite Platforms, https://www.utias-sfl.net/?page_id=89". Toronto, 2014.

[7] Robert D. Magner, *Extending the Capabilities of Terrestrial Target Tracking Spacecraft*. University of Toronto, 2018.